
Risk assessment of catastrophic failures in electric power systems

L. Mili* and Q. Qiu

Bradley Department of Electrical and Computer Engineering,
Virginia Polytechnic Institute and State University,
Alexandria Research Institute, Alexandria, VA 22314, USA
E-mail: lmili@vt.edu
*Corresponding author

A.G. Phadke

Virginia Tech., Blacksburg, Virginia, USA
E-mail: aphadke@vt.edu

Abstract: The declining reliability of the US electric power system is raising major concerns amongst both politicians and power engineers in the USA. One of the reasons put forward by the North Electric Reliability Council (NERC) is the detrimental role played by the protection systems during large disturbances, which tend to help the perturbations to propagate through over-tripping of fault free system components due to hidden failures. It turns out that the present practice in power transmission planning and online security analysis is to neglect the impact of the protection systems. In addition, the aim is to mitigate the vulnerability of the system to the loss of a single piece of equipment only by carrying out an N-1 security analysis. Consequently, the risk of cascading failures leading to blackouts and brownouts is neither assessed nor managed. This paper describes methodologies together with algorithms that assess the conditional risk of catastrophic failures in electric power networks due to hidden failures in protection systems. A catastrophic failure, defined as one that results in the outage of a sizable amount of load, may be caused by dynamic instabilities in the system or exhaustion of the reserves in transmission due to a sequence of line tripping leading to voltage collapse. Only the latter case is being considered. The aim of these algorithms is to identify the weak links in the systems, which are defined as those branches of the network whose tripping due to a fault lead to the highest probabilities of a catastrophic failure. The proposed methods are demonstrated on a 7-bus and a 61-bus system.

Keywords: risk assessment; cascading failures; hidden failures; weak links; electric power systems.

Reference to this paper should be made as follows: Mili, L., Qui, Q. and Phadke, A.G. (2004) 'Risk assessment of catastrophic failures in electric power systems', *Int. J. Critical Infrastructures*, Vol. 1, No. 1, pp.38–63.

Biographical notes: L. Mili is a Professor of Electrical and Computer Engineering at the Alexandria Research Institute of Virginia Tech. He received an Electrical Engineering Diploma from the Swiss Federal Institute of Technology, Lausanne, in 1976, and a PhD. from the University of Liege, Belgium, in 1987. Dr. Mili is a senior member of the Power Engineering Society of IEEE, the recipient of a 1990 NSF Research Initiation Award and of a 1992 NSF Young Investigator Award. His research interests include robust

statistics, statistics of extreme events, risk assessment and management, reliability analysis, power system analysis and control, and multifunction radar systems. Dr. Mili organised an NSF workshop dealing with the mitigation of the vulnerability of critical infrastructures to catastrophic events. The presentations and papers of this workshop are posted on a website [1].

Q. Qiu is presently completing his Ph.D. in Electrical Engineering at Virginia Tech. He obtained a BS from the Zhejiang University in 1989 and an MS. from the Graduate school of CEPRI in 1996, both being in electrical engineering. From 1989 to 1998 he was with CEPRI, China. His research interests include risk assessment of cascading failures in electric power systems, hidden relay failures, power system analysis and control.

A.G. Phadke is a University Distinguished Professor at Virginia Tech., in Blacksburg, Virginia. His primary research area is the microcomputer based monitoring, protection, and control of power systems. He is coauthor of two books on relaying: *Computer Relaying for Power Systems*, and *Power System Relaying*, and is the editor of and contributor to the book *Handbook of Electrical Engineering Computations*. He is a Fellow of IEEE and was awarded the IEEE Third Millennium Medal in 2000, named the Outstanding Power Engineering Educator by the IEEE in 1991, and received the Power Engineering Educator Award of the EEI in 1986. He received the IEEE Herman Halperin Transmission and Distribution award in 2000. He is the Chairman of the Technical Committee of USNC CIGRE, and Editor-In-Chief of IEEE Transactions on Power Delivery. Dr. Phadke was elected to the US National Academy of Engineering in 1993.

1 Introduction

Electric power systems are critical infrastructures in the same way as gas and oil networks, water networks, transportation networks, telecommunications and computer systems. These complex networked systems are increasingly interdependent on each other, as the digital society matures on a global scale. Consequently, their vulnerability and security are raising major concerns worldwide. For instance, the normal operation of water and telecommunications systems is maintained only if there is a steady supply of electrical energy. On the other hand, the generation and delivery of electric power cannot be ensured without provision to the power plants and power networks of fuel, water and various telecommunications and computer services for data transfer and control purposes. These interdependencies are strengthening their grip as the usage of the internet, intranet and other wide area computer networks is becoming prevalent.

The strong reliance of critical infrastructures on each other may turn a local disturbance in one of them into a large-scale failure via cascading events, which may have a catastrophic impact on the whole of society. Unfortunately, the risk of such a disastrous domino effect is growing in the USA because of the current trend to operate critical infrastructure systems closer to their stability or capacity limits. One compelling reason for this practice is, of course, economics. Providing these infrastructures with some degree of robustness comes at a price, which entails the achievement of the required level of redundancy in the equipment. This is all the more true since the

expansion of critical infrastructure systems does not keep pace with the rapid growth of demand.

A typical example of a critical infrastructure vulnerability that undergoes rising vulnerability to catastrophic failure is the electric power transmission network. There are several reasons for such a situation to prevail. Firstly, as witnessed in developed countries, including the USA, there has been a very slow expansion of the high voltage transmission grid during recent decades due to stringent regulations put forward in response to environmental concerns. Secondly, there are the profound structural reforms that the power industry has embarked on, which are geared toward the emergence and consolidation of competitive energy markets [2–6]. In Europe [3], South America [4], the Pacific [2], and now in North America [5,6], government institutions have issued new regulations to transform the vertically integrated utilities into independent generation, transmission, and distribution companies.

In these emerging competitive electricity markets, the wholesale market is the first to flourish and expand at a rapid rate, boosted by transmission's open access and the existence of a large variability in electricity prices between the US states. This price discrepancy has resulted in a growing amount of bulk power being transferred over long distances throughout the transmission grid, worsening a shortage of reserve margins in transmission that have prevailed since the mid 1980s. Consequently, blackouts and brownouts in the eastern and western parts of the country have been increasing in number at an alarming rate during recent years [7,8].

In bulk power transmission system planning and operation, the present practice is to carry out an N-1 contingency analysis [9]. Occasionally, an N-2 security analysis is employed in some stringent cases. However, it is implemented not via an exhaustive search but rather via a partial assessment of the system reserves over a small portion of the transmission network. An N-k security analysis for $k > 1$ is perceived as being impossible to achieve due to the huge number of cases that need to be investigated. In fact, under the assumption of independence between successive events, it would require checking the impact on the system reserve margins of the loss of every k out of N pieces of equipment, which yields a number of cases to be tested that grows exponentially with N. However, it is clear that this chain of contingencies are dependent on each other due to the protection-system interactions, either directly or indirectly via the changes in the distribution of power through the network or due to the possible multiple impacts of a triggering event, such as lightning or other natural hazards. Consequently, the probability of the occurrence of cascading failures is much higher than the probability of a random (i.e. independent) tripping of k out of N components of the system.

It is also the usual practice in reliability and security analysis to neglect the impact of the protection systems. As a result, cascading failures leading to blackouts or brownouts are not investigated. Until recently, large-scale blackouts were considered to be sufficiently rare events to be disregarded from the analysis. However, at least in the USA, ideas are evolving in this respect, prompted by the increasing number of major incidents that has plagued the US power systems since the mid 1990s. The frequency of major blackouts, which was about one per decade until 1996, has started to grow at an alarming rate since then [7,8]. For example, in July 1996, a series of blackouts struck the western part of the USA, leaving 2.2 million customers without electricity. One month later, islanding and blackouts affected eleven US western states and two Canadian provinces. In December 1998, the Bay area of San Francisco experienced a series of blackouts and in July 1999, it was the turn of New York City to suffer from the same type of cascading

failures. More recently, California has been struck by rolling blackouts initiated by the utilities to overcome a severe shortage of generation during peak hours. An exhaustive account of these blackouts can be found in the report prepared for the Transmission Reliability Program of the Department of Energy [8].

Besides the causes of the degradation of the power system reliability listed previously, there is the detrimental role played by the protection systems during large disturbances. As revealed by the study undertaken by the NERC over the period from 1984 to 1988 [9–12], in 73.5% of the significant disturbances that were investigated, undetected failures of the protection systems, termed hidden failures (HFs), have aggravated the disturbance by tripping fault free system components and, thereby, helped the perturbation to propagate further. One peculiarity of hidden relay failures is that they cannot be detected a priori, that is, they cannot be exposed before the system is perturbed. In particular, routine maintenance testing may not detect them or, even worse, may induce them by damaging relay components, as was the case in the 1977 New York blackout. Another source of HFs is the bad setting of relays. The present practice favours dependability at the expense of security, in that it ensures the isolation of a fault by allowing the tripping of fault free devices from time to time.

This paper describes methodologies together with algorithms that assess the risk of catastrophic failures in electric power networks. It builds on the pioneer work carried out by Thorp, Phadke, Horowitz and Tamronglak [11,12]. A catastrophic failure is here defined as one that results in the outage of a sizable amount of load, say 10% of the peak load. It may be caused by dynamic instabilities in the system or exhaustion of the reserves in transmission due to a sequence of line tripping leading to voltage collapse. Only the latter case is being considered. The aim of these algorithms is to identify the weak links in the systems, which are defined as those branches of the network whose tripping due to a fault lead to the highest probabilities of a catastrophic failure. Once the weak links are identified, they must be consolidated. To this end, a hidden failure monitoring and control system may be developed to supervise adaptive digital relays located in sensitive spots across the system. These relays may perform dynamic load shedding during an emergency state in conjunction with an adaptive splitting of the system that prevents the cascading failures from spreading throughout the network.

The paper is organised as follows. Section 2 unveils the mechanism of cascading failures in power systems due to hidden failures. Section 3 proposes a statistical method for estimating the probabilities of relay-hidden failures and system failures from historical data. Section 4 deals with the conditional risk assessment of system failure for a given generation and load profile and a given triggering event. Section 5 outlines variance-reduction Monte-Carlo methods to account for the variation of the generation and loading conditions of a power system. Section 6 provides a flowchart of subroutines that calculate the conditional risk of system failure and identify the weak links of a power system for a given generation and loading condition. Section 7 illustrates the application of the proposed methods on a 7-bus and a 61-bus system. Conclusions are provided in Section 8.

2 Cascading failures in power systems

2.1 Description of a typical scenario of cascading failures

One typical scenario of multiple contingencies leading to system failure is as follows: the triggering event is a short-circuit that occurs on one of the transmission lines of the system. The relays of that line send tripping signals to its circuit breakers. Before the faulted line opens, the short-circuit current is sensed by a certain number of relays located within *the region of influence* of the fault. The latter region is defined as the union of *the regions of vulnerability* of all the relays whose hidden failures are exposed by the fault. Consequently, each of these relays may unnecessarily open an unfaulted line if it suffers from a hidden failure. Hence, in addition to the faulted line, we may have two, three, or more simultaneous line openings, usually (but not necessarily) located in the vicinity of the fault. Consequently, the power that used to pass through the tripped lines finds its way through other links in the network, which in turn may overload some of them. If any of the overload currents is larger than the setting of the overcurrent relays, then the latter will open the associated unfaulted line, putting additional stress on the network. As a domino effect, this sequence of line tripping followed by line overloading may propagate throughout the network until either the line overloading vanishes or the stability limits or voltage collapse limits are reached. It is clear that these chains of contingencies are dependent on each other. In addition, several of them may cascade simultaneously. Consequently, the probability of these cascading failures occurring is much higher than the probability of a random (i.e. independent) tripping of k out of N components of the system.

It is interesting to note that a system failure consists of a sequence of cascading line tripping that originates from the faulty line and spreads sequentially from one location to another over an increasingly larger region of the network. A system failure also consists of the repetition of the same basic structure, which is the opening of few lines located in the same neighbourhood. This basic pattern repeats itself regardless of the size of the system failure, that is, regardless of whether it is a minor event that affects a small sub-network or a major event that results in the collapse of large segments of the network with dramatic consequences for millions of customers. To put it differently, a system failure exhibits a *self-similar* geometric shape [13].

At this point, the question that arises is the following: Where to reinforce the network in order to confine the cascading failures to a small region? It is clear that failures will propagate via the *weakest links* in the system. The latter may be defined as those lines of the network for which the probability of overloading and/or hidden relay failures is the largest. They are termed *hot spots* in the area of risk assessment and mitigation. A good analogy can be found in transport networks. Here, the hot spots include tunnels through mountains or heavily loaded roads that pass through urban areas.

2.2 Analysis of the 1977-New-York blackout

A typical example of hidden failures that played havoc with a power system is provided by the 1977-New-York blackout [14–17]. As shown in Figure 1, the New York power system was connected to the northern neighbouring systems through five 345-kV tie lines, which imported a total power of 3375 MW. It was connected from the south to the

summary, two relay-hidden failures contributed to the New York blackout. Although no hidden failure in the reclosing of relays occurred in the 1977 New-York blackout, it did happen in other system failures according to statistics reported by the IEEE/PSRC Working Group 13 [17].

3 Probability estimation of catastrophic failures from historical data

3.1 Probability estimation of hidden relay failures

Now, how to assess the probability of a system failure? Obviously, it is based on the estimation of the probabilities of hidden relay failures. We propose the following approach to estimate these probabilities from historical data. First, the relays are grouped into statistically homogenous classes with respect to their failure rates. Specifically, the relays are classified according to their type, their technology and their age. The relay types are very diverse; they include distance relays, pilot relays, overcurrent relays, bus relays, transformer relays and excitation relays, to cite a few. In addition, it is important to distinguish electromagnetic relays from electronic relays and computer relays. Finally, age also matters because the failure rate during the debugging phase of a newly installed relay may be different from those of the mature operating phase and the wear out phase of this relay. The failure rate is expected to be high during the early and late operating periods and lower during the mature period of the relay. In other words, the reliability-aging curve of the relay has the well-known bathtub shape [9]. This may be especially true for electronic and computer relays.

Once the relay classification is performed, we may investigate a sample of relay-related events that have occurred in the US transmission network. It is important that this sample, denoted by S , be representative of the whole population of events. To this end, the events will be randomly selected. Obviously, they will have a broad range of degrees of severity. If the randomisation is carried out properly, the sample S will thus include mild events that have little or no consequences, average events that have some impact, and extreme events with catastrophic implications. It is anticipated that the mild events form the bulk of system failures while the catastrophic events are rare; they have a very low probability of occurrence.

The probabilities of hidden relay failures are estimated as follows: consider a given relay class, say the i -th class. Let n_i denote the total number of the relays of that class involved in all the events of the sample S . Let m_i denote the total number of these relays whose hidden failures have been exposed. Then, an estimate of the probability p_i of hidden failures of the i -th relay class is defined as $p_i = m_i / n_i$.

3.2 Probability estimation of catastrophic failures

The probability of catastrophic system failures can be estimated from the sample S of relay related events. To this end, we need to define a measure of severity of a system failure. Let X be such a measure. X may be defined as the cost in dollars suffered by the customers or the energy in MWh not delivered. X can be regarded as a random variable that takes a broad range of values, varying from zero to thousands of MWh. The probability distribution function of X may be estimated from the sample S . Specifically, a histogram can be derived and an empirical density function estimated from that sample.

Hence, estimates of the probabilities of catastrophic events are given by the relative frequency of very large values of X . These probability estimates are very small and located in the tail of the probability density function.

3.3 Confidence interval estimation based on the bootstrap method

The confidence intervals of both the probabilities of hidden failures and of catastrophic system failures may be estimated by means of the nonparametric bootstrap method [18,19]. It is a computationally intensive method that is based on the concept of sampling distribution. To explain this concept let us consider a parameter of a population probability distribution, γ , to be estimated by means of an estimator Γ using a sample drawn from that population. The sampling distribution of Γ can be thought of as the relative frequency distribution of all possible values taken by Γ calculated from an infinite number of random samples of finite size drawn from the population of the Γ values [18]. It is the estimate of this sampling distribution that allows us to make inferences on the parameter γ from the estimator Γ . The objective here is to estimate confidence intervals in which the true value of γ lies with a high probability.

While traditional parametric inference utilises strong assumptions about the probability distribution of Γ , which is usually assumed to be normally distributed, the nonparametric bootstrap is distribution free, that is, no a priori distribution of Γ is made. The bootstrap method relies on the fact that the sampling distribution of Γ is a good estimate of the population distribution. How is this sampling distribution built? It is carried out by using Monte Carlo sampling, where a large number of samples of size n , called resamples, are randomly drawn with replacement from the original sample. Although each resample will have the same number of elements as the original sample, it may include some of the original data points more than once, while some others are not included. Therefore, each of these resamples will randomly depart from the original sample. Because the elements in these resamples vary slightly, the statistic Γ^* , calculated from one of these resample, will take on slightly different values. The central assertion of the bootstrap method is that the relative frequency distribution of these Γ^* 's is an estimate of the sampling distribution of Γ .

The main steps of the nonparametric bootstrap procedure can be stated more formally as follows [18,19]. Consider a sample of values taken by a random variable, say the probability estimates previously defined. Let n be the size of this sample, called the original sample. Then, apply the following steps:

- Step 1. From the original sample, draw M random samples of size n with replacement to obtain M resamples. The practical size of M depends on the statistical method to be applied to the sampling distribution. Typically, M is at least equal to 1000 when a confidence interval estimate of Γ is to be calculated.
- Step 2. For each resample, calculate the statistic of interest, Γ^* . This may be the mean, the median or the mode estimator, or any other location or scale statistic.
- Step 3. Order the M estimates of Γ^* by increasing values and assign a probability of $1/M$ to each of them. Identify the $[(1 - \alpha/2) M]$ -th and the $[(\alpha/2) M]$ -th quantiles of the sampling distribution, where α is a given level of confidence, say 0.95, and $[x]$ denotes the largest integer smaller than the real number x . These

quantiles are the lower and upper limits of the α -level confidence interval of the estimator Γ .

4 Risk assessment of system failure for a given generation and load profile

The conditional risk of system failure is defined as the product of the conditional probability of system failure by its severity. System failure here represents either a collection of load outages or a voltage collapse. Assuming that the probabilities of hidden failures are known, we describe a method that calculates the conditional probability of system failure for a given generation and load profile and for a given triggering event. The latter is a short-circuit on a piece of equipment of the transmission network, such as a line, a transformer, a bus or a generator

4.1 Conditional probability calculation of system failure

The proposed methodology is based on an event tree [20] that allows us to calculate the conditional probability of system failure. The event tree related to cascading outages due to a fault on a line, say line i , is depicted in Figure 2. It consists of a collection of events that occur in sequence as follows. Firstly, the triggering event may be a permanent or a temporary fault with a probability $P_{Fi} P_{Pi}$ and $P_{Fi} (1 - P_{Pi})$, respectively, where P_{Fi} is the probability of a fault and P_{Pi} is the conditional probability that the fault is permanent. Once the fault occurs, the circuit breakers of the faulty line should open to clear the fault. However, they may remain stuck in a closed position with a conditional probability P_{Bi} as shown in [21].

In the event of a temporary fault, the breakers should reclose after a brief instant, an event that may fail to occur with a conditional probability P_{Ri} . In addition to the relays of the faulty line, other relays may also sense the fault current. Unlike the former relays, the latter should block their tripping mechanisms and not open the lines under their control. However, one or several of them may each suffer from a hidden failure with a small probability P_{Hi} and, thereby, trip the associated non-faulty line. This sequence of line tripping may result in either a system failure or line overloads. In the latter case, another sequence of line tripping, due to hidden relay failures, may lead to system failure or to line overloads and so forth. Consequently, the probability of system failure is written as:

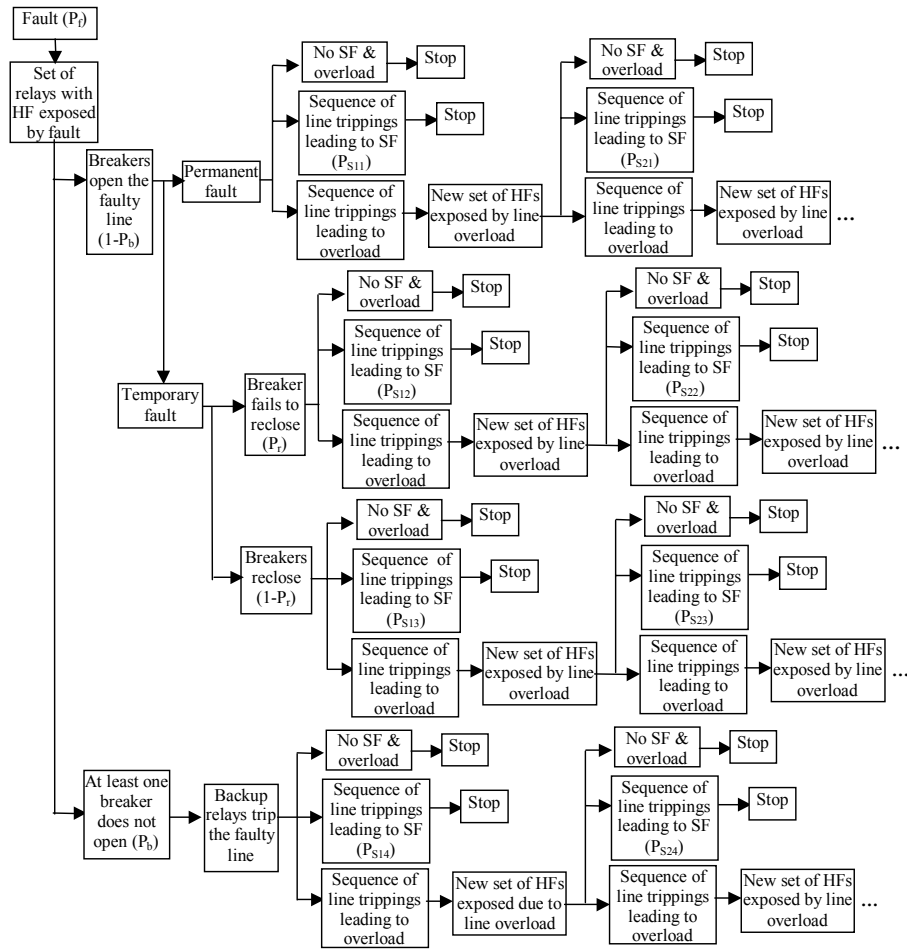
$$P_{Si} = P_{Fi} (1-P_{Bi}) \{P_{Pi} (P_{HPi} + P_{LPi}) + (1- P_{Pi}) [P_{Ri} (P_{HTNi} + P_{LTNi}) + (1- P_{Ri}) (P_{HTRi} + P_{LTRi})]\} \quad (1)$$

where:

- P_{Bi} : probability that a circuit breaker of the faulty line i does not open in time
- P_{Ri} : probability that the circuit breakers of the faulty line i do not reclose following a temporary fault
- P_{HPi} : probability of system failure due to hidden relay failure, given the occurrence of a permanent fault
- P_{HTNi} : probability of system failure due to hidden relay failure, given the occurrence of a temporary fault and the non-reclosing of the faulty line

- P_{HTRi} : probability of system failure due to hidden relay failure, given the occurrence of a temporary fault and the successful reclosing of the faulty line
- P_{LPI} : probability of system failure due to line overloads, given the occurrence of a permanent fault
- P_{LTNi} : probability of system failure due to line overloads, given the occurrence of a temporary fault and the non-reclosing of the faulty line
- P_{LTRi} : probability of system failure due to line overloads, given the occurrence of a temporary fault and the reclosing of the faulty line.

Figure 2 Event tree for probability evaluation of cascading failures



SF: System failure, HF: Hidden failure

Let us now derive the expression of the probability of system failures given a permanent fault, which is denoted by P_{HPI} . To this end, let us define S_C as the set of all sequences of line outages leading to system failure due to hidden failures exposed by the short-circuit current. Let us also define P_j as the probability of the j -th sequence. Then, obtain:

$$P_{HPi} = \sum_{j \in S_C} P_j . \quad (2)$$

The probability P_j is the product of:

- 1 the probabilities $\{p_m$ for all $m \in S_{CTj}\}$ of all tripped lines in the j -th failure mode leading to system failure, which form the subset S_{CTj} of S_C ,
- 2 the probabilities $\{(1-p_n)$ for all $n \in \bar{S}_{CTj}\}$ of all the remaining lines that do not trip, which form the subset \bar{S}_{CTj} of S_C . Hence, we get:

$$P_j = \sum_{j \in S_C} \left\{ \prod_{m \in S_{CTj}} p_m \prod_{n \in \bar{S}_{CTj}} (1-p_n) \right\} , \quad (3)$$

where

$$S_C = S_{CTj} \cup \bar{S}_{CTj} . \quad (4)$$

Similarly, we can derive the expressions of P_{HTNi} and P_{HTRi} as well as the expressions of the probabilities of system failure due to line overloads, P_{LPi} , P_{LTNi} , and P_{LTRi} . For example, we have:

$$P_{LPi} = \sum_{j \in S_L} P_j , \quad (5)$$

where

$$P_j = \sum_{j \in S_L} \left\{ \prod_{m \in S_{LTj}} p_m \prod_{n \in \bar{S}_{LTj}} (1-p_n) \right\} , \quad (6)$$

and

$$S_C = S_{CTj} \cup \bar{S}_{CTj} . \quad (7)$$

Here, S_L is the set of all sequences of line outages leading to system failure due to hidden failures exposed by line overloads, and S_{LTj} is the subset of S_L that consists of all tripped lines in the j -th failure mode leading to system failure. Also, p_m denotes the probability that line m trips due to a hidden failure exposed by line overloads.

For a large power system, it is a formidable task to evaluate the probability of system failure induced by a fault on every branch of the network. Consequently, a fast screening method must be used beforehand to identify the regions of the network that may include weak links. These regions are likely to be those with the smallest reserves in transmission and/or in generation. To pinpoint them, a continuation-power-flow calculation may be

applied, as explained in Section 6. Note that the *weak links* are the *minimal cut sets* of the event tree, in that they lead to system failure with the smallest number of line trippings, which in turn results in the highest probabilities of system failure.

4.2 System failure significance

Once the conditional probability of system failures have been evaluated, it is important to assess the risk of system failure given a triggering event, T_i , which is defined as:

$$Risk = P_i S_i w_i, \quad (8)$$

where P_i denotes the probability of system failure, S_i is a measure of severity of system failure, and w_i is a weight coefficient. The severity of system failure can be represented by: the number of customers disconnected, the amount of power curtailed, the amount of energy not delivered, or the amount of dollars lost by the customers. The weight coefficient accounts for the relative importance of a tripped load or a disconnected substation. Obviously, hospitals, governmental buildings and major industries should be assigned more weight than residential customers.

5 Risk assessment of system failure for planning

It is clear that the severity of a system failure depends heavily on the load and generation profiles that are considered. Accounting for the variation of the generation and load profile is required for a planning study. Since it is impossible to process all the system operating conditions, we may resort to a sampling approach by investigating a large sample of the operating conditions, a technique known as Monte Carlo-based production simulations [9]. Their objective is to meet the system load demand at minimum operating cost while satisfying the security constraints of the system. Typically, four types of generating units are considered, each of which has its specific operating characteristics. These are hydro-station, pumped-storage station, thermal unit and nuclear unit. To account for the forced outages of a dispatched unit, a random number ranging from 0 to 1 is generated for each unit in a priority list ranked by operating cost. If the generated random number is greater than the forced outage rate of a unit, then the latter is deemed to be available for service; otherwise it is unavailable and the next unit in the priority list is checked for availability in the same way. As pointed out by Stoll [9], Monte Carlo methods do not need to be executed on an hourly basis. In general, the unit's state (on outage or in service) is assumed to remain unchanged during a whole week, an assumption that greatly reduces computing time.

In assessing the risk of catastrophic failures, the transmission losses may be neglected while the operation and maintenance costs are not considered separately. The latter may be reflected in the fuel cost instead. Other operating constraints may not be included in this analysis, such as the unit minimum uptime/downtime rules. In summary, the long-term planning simulation includes the following steps:

- 1 give the first priority to the must-run units serving the security purpose (the area protection rule)
- 2 dispatch the units with the minimum cost in the priority list (the economic criteria)
- 3 observe that the sum of the minimum technical ratings of all committed thermal units does not exceed the minimum daily load, while ensuring that the sum of the maximum ratings of the committed units meets the maximum daily load plus the reliable spinning reserve (the technical requirements)
- 4 ensure that the interchanging power between two zones does not exceed the capacity limit of the tie lines.

To speed the calculations up further, variance-reduction methods may be applied. The reader is referred to Rubinstein [22] and Cochran [23] for a general account of these methods. In power systems, Thorp *et al.* [12] advocate the use of importance sampling to identify the weak links of a transmission network. Oliveira *et al.* [24] showed that control variates significantly reduce the number of samples in Monte Carlo-based composite power system reliability evaluations. Billinton and colleagues applied importance sampling [25], stratified sampling [26], and antithetic variates [26,27] to efficiently calculate various reliability indices for composite power systems. They found that antithetic variates outperform the other methods [27]. Marnay and Strauss [28] compare antithetic and stratified sampling when estimating chronological production hourly marginal cost. They recommend the use of a procedure that combines antithetic sampling and proportional stratification.

A much simpler alternative method would be to consider only different load-generation profiles, as listed in Table 1. To be specific, the study is carried out for two seasons; namely, the summer and the winter seasons, which have significant differences with respect to the load-generation profile. For each season, three load conditions (most frequently load, peak and off-peak load) are selected and three different generation profiles under each load condition are considered. Hence, for each year, a total of 18 cases are evaluated, the only requirement being that they cover a broad range of operating conditions of the power system under investigation.

Table 1 Load-generation profiles

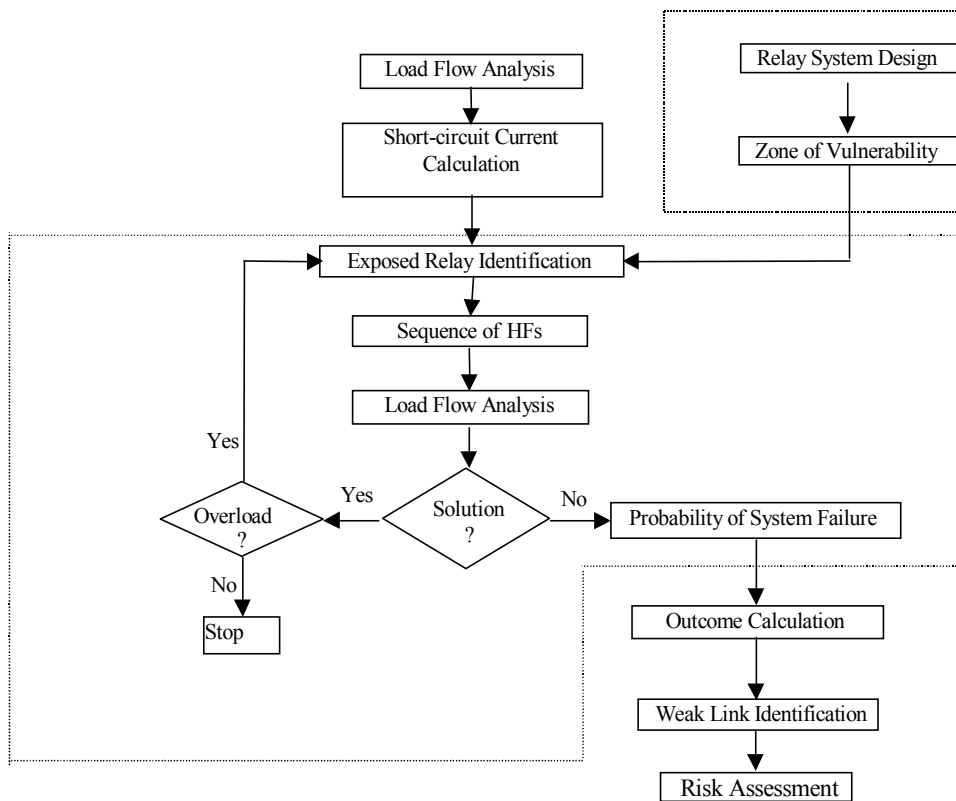
<i>Load profile</i>	<i>Generation profile</i>	<i>Load profile</i>	<i>Generation profile</i>
Summer		Winter	
	Normal case		Normal case
Peak load	Worst case	Peak load	Worst case
	Alternative case		Alternative case
	Normal case		Normal case
Off-peak load	Worst case	Off-peak load	Worst case
	Alternative case		Alternative case
	Normal case		Normal case
Most frequent load	Worst case	Most frequent load	Worst case
	Alternative case		Alternative case

6 Algorithms for the probability calculation of cascading failures

6.1 General description of the risk-assessment algorithms

Based on the foregoing outlined methodology, a package of software programs has been developed. It includes a continuation-power-flow program, a short circuit program, a power-flow program, and a cascading-failure-probability-calculation program. These programs are run sequentially, as depicted in Figure 3. In the first step, the continuation power flow program is executed to identify the heavy loaded regions of the system with the smallest reserve margins. Cascading failures in these regions are likely to occur with the highest probability, since few line trippings due to hidden relay failures may result in the disconnection of large segments of the load. In the second step, a three-phase short-circuit is applied sequentially to every branch of these regions and, in each case, all those relays that are seeing a large short-circuit current are pinpointed via the short circuit program. Then, for every combination of relay trippings, all the lines that become overloaded are singled out through the power flow program. The hidden failures of their relays may be exposed, resulting in the tripping of another set of lines, and so forth. This sequence of events continues until either a sufficiently large amount of load is being disconnected or a voltage collapse has occurred. In the last step, the probability of system failure is calculated.

Figure 3 Flowchart of the risk assessment algorithm of catastrophic failure



6.2 *A fast screening method based on the continuation-continuation-power flow*

As a fast screening, a continuation-power-flow program is executed to identify the regions that have the smallest reactive reserves in the system. Starting from a power flow solution, say at peak load, the algorithm traces the power flow solution curves as the reactive power injections of the load buses are increased up to the saddle-node bifurcation point [29,30]. The latter is defined as the point where the power flow Jacobian matrix becomes singular, also termed the point of voltage collapse.

Several continuation schemes have been proposed in the literature for power system applications [30-32]. In this study, we used the predictor-corrector scheme initiated by Rubicek and Marek [33] in conjunction with the local parametrisation method proposed in [34] for the prediction step. The predictor finds a point along the tangent of the V-Q curve in the direction of the saddle-node bifurcation point while the corrector uses this point as an initial condition to seek, via a Newton-Raphson algorithm, a solution to a set of parametrised power flow equations.

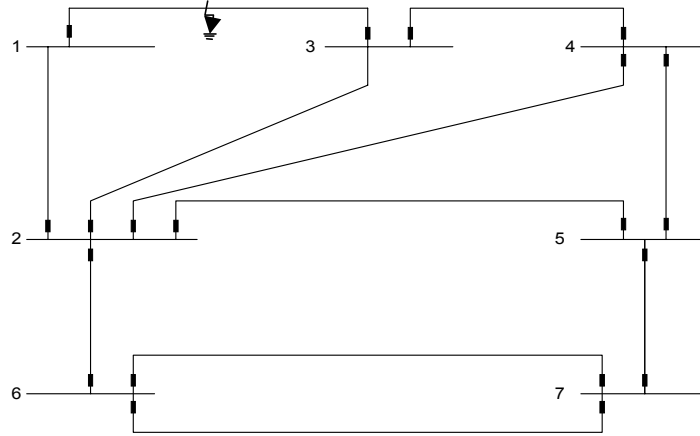
7 **Simulation results**

7.1 *Simulation results obtained on a 7-bus system*

The mechanism of cascading failures represented by the event tree is illustrated on a 7-bus system, whose one-line diagram is shown in Figure 4. Here, we assume that the network is protected only by zone 1, zone 2 and zone 3 distance relays. The setting specifications proposed in [35] are equal to 70% and 120% of the protected line for zone 1 and zone 2 relays, respectively, and 100% of the protected line length plus 120% of the longest adjacent line for zone 3 relays. In this example, we also made the following assumptions:

- 1 the triggering event is a permanent three-phase short-circuit on lines 1-3, which occurs with a probability P_f
- 2 the faulty line is opened by its own circuit breakers, that is, there is no breaker stuck in the closing position
- 3 all the relays have the same hidden failure probability denoted by P_{HF}
- 4 the hidden failure of a relay is exposed whenever the associated line is overloaded
- 5 a system failure is supposed to occur whenever at least one bus is isolated from the rest of the network.

By using a short-circuit and a load flow program, we determine the list of cascading events on a power system following a legitimate tripping of a given line. The short-circuit program is run to identify all the exposed relay hidden failures and a load flow calculation is executed to identify the new set of relays whose hidden failures have been exposed due to overloaded lines.

Figure 4 One-line diagram for the 7-bus test system

The settings of all the zone 3 relays are shown in Table 2, where R_{ij} denotes the relay at the i th end of line $i-j$. Suppose that a three-phase fault is applied to the bus-3 end of line 1-3. We calculate the short-circuit current at the fault point by assuming that all the pre-fault bus voltages are equal to 1 p.u. Then, we determine the voltage drops at all the buses. Using the principle of superposition, we obtain the fault-on voltages, which allow us to calculate the short-circuited current on every branch of the network. Finally, we determine the apparent impedance seen by each relay. Table 3 displays the zone 3 relays, with hidden failures exposed to fault. The flow chart of the general procedure to identify an exposed relay is displayed in Figure 3. The apparent impedances seen by them are smaller than their settings. As a result, these relays may trip incorrectly. The voltages, short-circuited currents, and apparent impedances of the exposed relays are also listed in Table 3. In the final step, a load flow program is executed to identify the overloaded lines following the tripping of those lines with exposed relay hidden failures and the probabilities of system failure are calculated.

Table 2 Settings of zone-3 distance relays

<i>Relay</i>	<i>Setting (p.u.)</i>	<i>Relay</i>	<i>Setting (p.u.)</i>
R ₁₂	0.276	R ₂₁	0.348
R ₁₃	0.456	R ₃₁	0.312
R ₃₄	0.318	R ₄₃	0.318
R ₄₅	0.384	R ₅₄	0.456
R ₅₇	0.348	R ₇₅	0.348
R ₂₃	0.468	R ₃₂	0.398
R ₂₄	0.468	R ₄₂	0.398
R ₂₅	0.408	R ₅₂	0.338
R ₂₆	0.348	R ₆₂	0.276
R ₆₇	0.312	R ₇₆	0.312

Table 3 List of exposed zone 3 relays

<i>Exposed relay</i>	<i>Setting (p.u.)</i>	<i>Apparent impedance</i>	<i>Voltage (p.u.)</i>	<i>Current (p.u.)</i>
R ₂₃	0.468	0.18	0.5205	2.89
R ₂₄	0.468	0.3025	0.52052	1.72
R ₄₃	0.318	0.03	0.2108	1.4
R ₅₄	0.456	0.3905	0.547	7.02

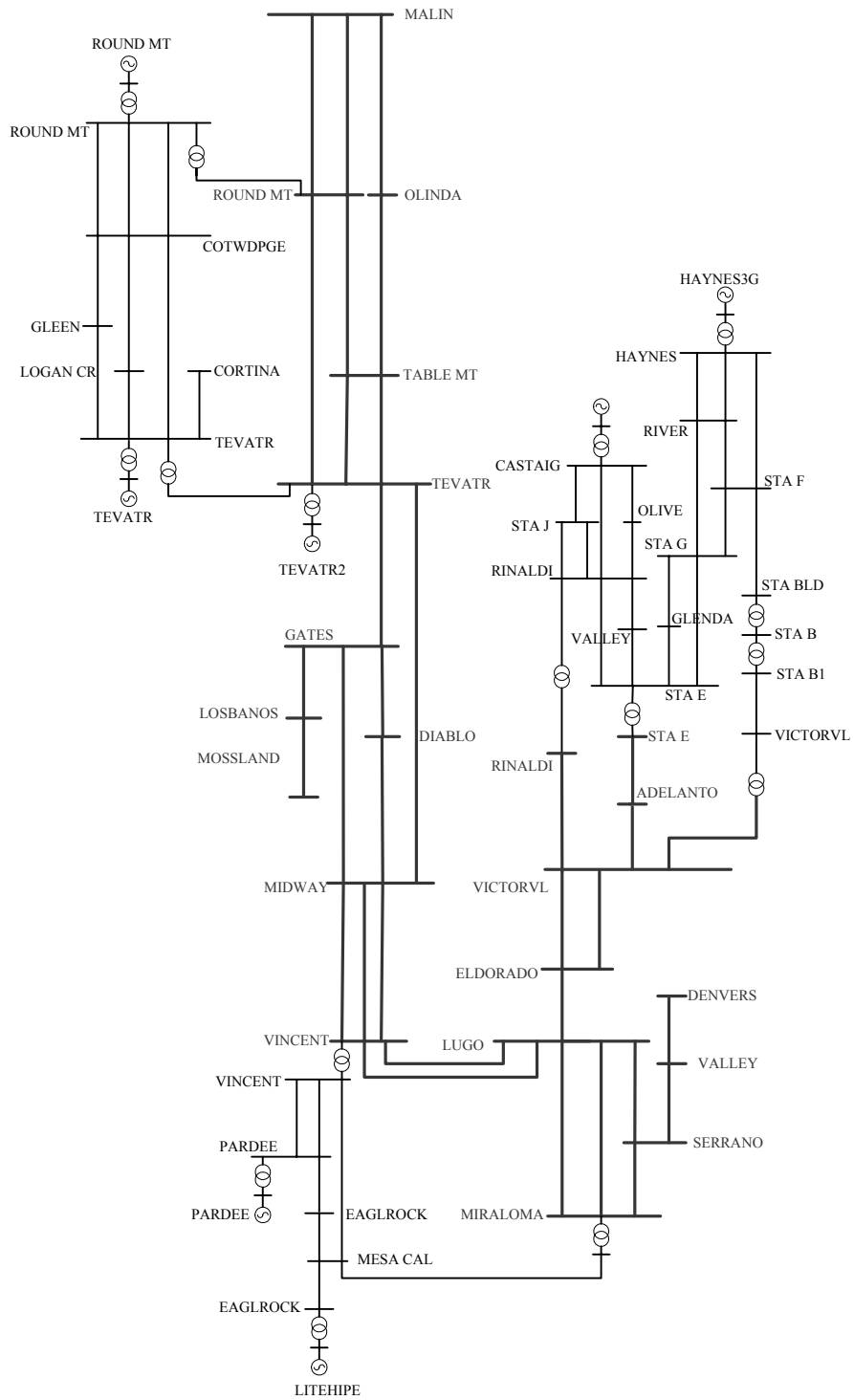
The simulation results are displayed in Table 4. Note that the lines exposed to hidden failures can trip individually or simultaneously, as shown in the second column of Table 4, which is entitled Step 2. Also, note that the steps of a sequence of trippings are numbered 1 to 6. For example, in the tripping sequence of case 1, line 2-3 opens due to a hidden failure in step 2, which in turn induces line 3-4 to be overloaded and to disconnect in step 3. Finally, line 2-5 trips for the same reason in step 4. Since no overloaded line is encountered after step 4, the line tripping sequence will stop. In some cases, there may be more than one line overloaded at the same time due to previous contingencies. For example, both lines 3-4 and 2-5 are overloaded in step 3 of case 5; they will trip simultaneously at this step.

Table 4 Probabilities of cascading failure for the 7-bus system

<i>Sequence</i>	<i>Step 2</i>	<i>Step 3</i>	<i>Step 4</i>	<i>Step 5</i>	<i>Step 6</i>	<i>Probability of System Failure</i>
<i>Case</i>	<i>Line tripping(s) due to HF</i>	<i>Line tripping(s) due to overload</i>	<i>Line tripping(s) due to overload</i>	<i>Line tripping(s) due to overload</i>	<i>Line tripping(s) due to overload</i>	
1	2-3	3-4 (117%)	2-5 (102%)			$P_f P_{HF} P_{34} P_{25}$
2	2-4					$P_f P_{HF}$
3	3-4	2-3 (174%)	2-5 (102%)			$P_f P_{HF} P_{33} P_{25}$
4	5-4					$P_f P_{HF}$
5	2-3 & 2-4	3-4 (117%) 2-5 (140%)	2-6 (108%)	5-4 (120%)		$P_f P_{HF}^2 P_{34} P_{25} P_{26} P_{54}$
6	2-3 & 4-3	2-5 (102%)				$P_f P_{HF}^2 P_{25}$
7	2-3 & 5-4	3-4 (117%)	2-5 (113%)			$P_f P_{HF}^2 P_{34} P_{25}$
8	2-4 & 3-4	2-3 (174%)	2-5 (132%)	2-6 (108%)	5-4 (120%)	$P_f P_{HF}^2 P_{23} P_{25} P_{26} P_{54}$
9	2-4 & 5-4					$P_f P_{HF}^2$
10	3-4 & 5-4	2-3 (174%)	2-5 (113%)			$P_f P_{HF}^2 P_{23} P_{25}$
11	2-3&2-4&3-4	2-5 (132%)	2-6 (108%)	5-4 (120%)		$P_f P_{HF}^3 P_{25} P_{26} P_{24}$
12	2-3&2-4&5-4	2-5 (127%)	2-6 (108%)			$P_f P_{HF}^3 P_{25} P_{26}$
13	2-3&3-4&5-4	2-3 (113%)				$P_f P_{HF}^3 P_{23}$
14	2-4&3-4&5-4	2-3 (174%)	2-5 (127%)	2-6 (108%)		$P_f P_{HF}^3 P_{23} P_{25} P_{26}$

The system failure probabilities are given in the last column of Table 4. Here, P_{ij} denotes the conditional probability that the overloaded line ij is mis-tripped. We observe from Table 4 that there are 14 sequences of line tripping that lead to a system failure.

Figure 5 One-line diagram of the California sub-system

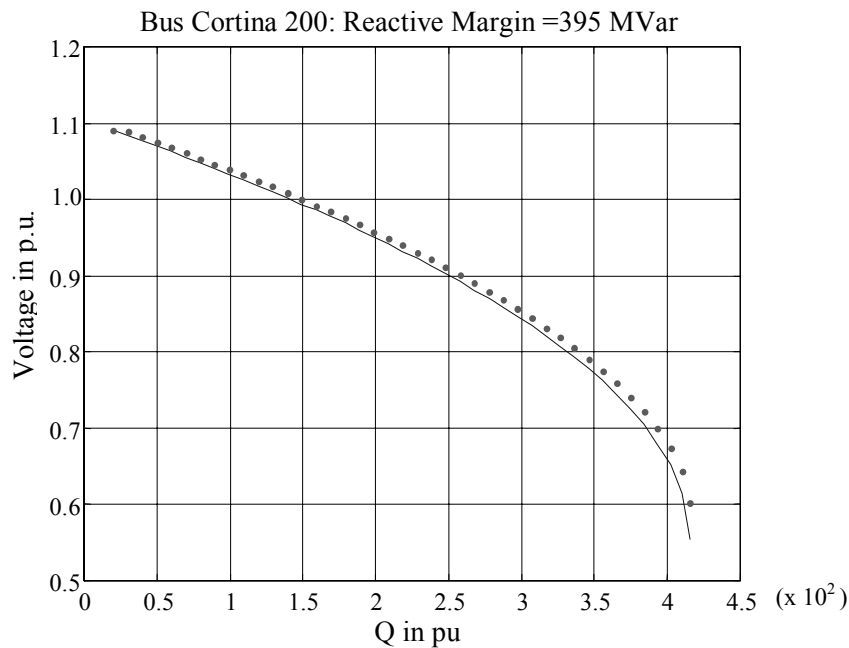


7.2 Simulation results performed on the California 61-bus subsystem

The software programs that implement the proposed methodology have been applied to the California subsystem of the WSCC 179-bus reduced system. Its one-line diagram is sketched in Figure 5. This subsystem includes 61 buses and 83 branches at the voltage levels of 500kV, 230kV, and 110kV and serves a total load of 21,576 MW. The main area of this sub-network is the tightly connected Los Angeles area that comprises 41 buses and 52 branches.

The objective here is to assess the risk of catastrophic failure of this subsystem. A major failure is defined as being either a loss of a large amount of load, say larger than 1000 MW, or a voltage collapse. To this end, the continuation power flow was first executed sequentially at each of the 34 load buses of the subsystem to assess their respective reactive power margins to voltage collapse. As an example, Figure 6 displays the Q-V curve of Bus 34, named Cortina 200, whose reactive reserve was found to be equal to 395 MVar. The reserve margins grouped by voltage level while being ordered by ascending magnitude are listed in Table 5. In other words, for every voltage level, the buses with the smallest reserves are located at the top of the list. Therefore, the areas in their vicinities are likely to include the weak links of the subsystem.

Figure 6 Q-V curve at Bus 34, named Cortina 200



As a second step of the method, a three-phase short circuit is applied and a short-circuit calculation is carried out for every branch of the California subsystem. This calculation allows us to identify the exposed relay hidden failures, which are listed in the third column of Table 6. Let p_f denote the probability of a three-phase short-circuit on a given branch and let p denote the probability of an exposed relay hidden failure that will trip the

associated line. For $q = 1 - p$, $p_f = 10^{-3}$, and $p = 10^{-4}$, the probabilities of catastrophic failure are calculated and their values listed in Table 6. We observe that they range from 10^{-3} to 0. Note that all but cases 10, 14, and 15 lead to voltage collapse. While case 10 results in a loss of load of 1230 MW, cases 14 and 15 do not lead to a catastrophic failure. It is observed that the weak links of the California subsystem are the first 8 branches listed in Table 6, since the highest probabilities of voltage collapse are associated with them. It turns out that the first seven of these branches are tie lines of the California subsystem, five of them being heavily loaded.

Table 5 Voltage stability margins at the load buses of the California sub-system

<i>Bus No.</i>	<i>Bus name</i>	<i>Voltage (kV)</i>	<i>Base case ($\times 10^2$ MW, $\times 10^2$ MVar)</i>	<i>Margin $\times 10^2$ MVar)</i>	<i>Margin from the base case ($\times 10^2$ Mvar)</i>
44	LUGO	500	-9.07+j0.952	8.35	7.40
31	VALLEY	500	4.06+j0.41	11.50	11.09
6	LOSBANOS	500	2.65+j0.14	17.80	17.66
13	ROUND MT	500	-19.2-j0.94	19.50	20.44
30	SERRANO	500	12.3+j0.728	28.50	27.77
36	ADELANTO	500	-18.62+j0.59	29.90	29.31
27	VICTORVL	500	0.0+j0.0	31.50	31.50
3	GATES	500	3.05+j0.834	33.00	32.17
18	TEVATR	500	56.61+j19.91	66.10	46.19
24	MIRALOMA	500	30.98+j7.89	60.10	52.21
26	VICTORVL	287	-1.69+j1.402	10.15	8.75
53	STA BLD	230	1.38+j0.28	13.45	13.17
43	EAGLROCK	230	1.75+j 0.18	15.60	15.42
56	STA F	230	1.17+j0.24	17.20	16.96
49	RIVER	230	3.2+j0.65	18.40	17.75
40	GLENDAL	230	1.35+j0.2	19.05	18.85
57	STA G	230	1.21+j0.25	20.90	20.65
61	VALLEY	230	2.052+j0.176	23.80	23.62
45	OLIVE	230	-0.728-j0.17	24.10	24.27
54	STA E	230	8.078+j1.321	26.10	24.78
22	MESA CAL	230	3.774+j0.645	25.60	24.96
58	STA J	230	8.877-j0.062	27.60	27.66
33	VINCENT	230	10.66+j1.79	34.50	32.71
47	RINALDI	230	1.21+j0.25	35.30	35.05
59	SYLMARLA	230	-27.71-j4.92	30.80	35.72
60	SYLMAR S	230	4.01+j0.806	37.00	36.19
29	PARDEE	230	31.18+j0.78	41.10	40.32
20	LITEHIPE	230	31.91+j6.3	73.40	67.10
34	CORTINA	200	-0.443+j0.2	4.15	3.95
35	COTWDPGE	200	2.104-j0.77	10.70	11.47
12	ROUND MT	200	1.48+j1.18	21.00	19.82
16	TEVATR	200	8.84+j0.868	32.50	31.63
8	MIDWAY	200	7.776+j1.626	37.25	35.62
50	STA B	138	2.372-j0.632	10.00	10.63

Table 6 Probability of voltage collapse due to a fault on major 500kV transmission lines in the California subsystem

<i>No. Faulty line</i>	<i>Lines with exposed hidden relay failures</i>	<i>Probability of voltage collapse</i>	<i>Probability of VC for $p_f=10^{-3}$, $p=10^{-3}$.</i>
1 MALIN – OLINDA	MALIN SUMMER L GRIZZLY MALIN (1) GRIZZLY MALIN (2) MALIN ROUND MT (1) MALIN ROUND MT (2)	$p_f(1-3pq^4)$	$\approx 10^{-3}$
2 OLINDA – TEVATR	TEVATR MIDWAY GATES TEVATR TABLE MT TEVATR (1) TABLE MT TEVATR (2) MALIN OLINDA	$p_f(1-q^5)$	$\approx 10^{-3}$
3 TABLE MT – TEVATR (1)	ROUND MT TABLE MT (1) ROUND MT TABLE MT (2) TABLE MT TEVATR (2) GATES TEVATR MIDWAY TEVATR OLINDA TEVATR	$p_f(p+pq+p^2q^2+p^2q^4) \approx 2 \times 10^{-7}$ $\approx p_f p (1+q)$	
4 MALIN – ROUND MT (1)	MALIN ROUND MT (2) ROUND MT TABLE MT (1) ROUND MT TABLE MT (2) GRIZZLY MALIN (1) GRIZZLY MALIN (2) MALIN SUMMER L MALIN OLINDA	p_f $(p+pq+p^2q^2(1+2p^2-p^3))$ $\approx p_f p (1+q)$	$\approx 2 \times 10^{-7}$
5 TEVATR – MIDWAY	OLINDA TEVATR TABLE MT TEVATR (1) TABLE MT TEVATR (2) GATES TEVATR MIDWAY DIABLO (1) MIDWAY DIABLO (2) MIDWAY GATES MIDWAY LOSBANOS MIDWAY VINCENT (1) MIDWAY VINCENT (2) MIDWAY VINCENT (3)	p_f $(p+pq+p^2q^2+p^4q^4+p^6q^5)$ $\approx p_f p (1+q)$	$\approx 2 \times 10^{-7}$

Table 6 Probability of voltage collapse due to a fault on major 500kV transmission lines in the California subsystem (continued)

No. Faulty line	Lines with exposed hidden relay failures	Probability of voltage collapse	Probability of VC for $p_f=10^{-3}$, $p=10^{-3}$.
6 TEVATR – GATES	TEVATR OLINDA	$p_r(p+pq+p^2q^2)$ $\approx p_r p (1+q)$	$\approx 2 \times 10^{-7}$
	TABLE MT TEVATR (1)		
	TABLE MT TEVATR (2)		
	TEVATR MIDWAY		
	GATES LOSBANOS		
	GATES MIDWAY		
	GATES DIABLO		
7 ROUND MT – TABLE MT (1)	MALIN ROUND MT (1)	$p_r(p+p^2q+p^2q^3)$ $\approx p_r p$	$\approx 10^{-7}$
	MALIN ROUND MT (2)		
	TABLE MT TEVATR (1)		
	TABLE MT TEVATR (2)		
	ROUND MT TABLE MT (2)		
8 MIRALOMA – SERRANO	SERRANO VALLEY	$p_r(p+p^2q)$ $\approx p_r p$	$\approx 10^{-7}$
	SERRANO LUGO		
	MIRALOMA LUGO (1)		
	MIRALOMA LUGO (2)		
9 VALLEY – DEVERS	DEVERS PALOVRDE (1)	$p_r p^2$	$\approx 10^{-11}$
	DEVERS PALOVRDE (2)		
	VALLEY SERRANO		
10 SERRANO – VALLEY	VALLEY DEVERS	$p_r p^2$	$\approx 10^{-11}$
	SERRANO LUGO		
	SERRANO MIRALOMA		
11 VINCENT – LUGO (1)	VINCENT (1) MIDWAY	$p_r(p^3+p^3q)$	$\approx 2 \times 10^{-15}$
	VINCENT (2) MIDWAY		
	VINCENT (3) MIDWAY		
	LUGO VINCENT (2)		
	LUGO ELDORADO		
	LUGO MIRALOMA (1)		
	LUGO MIRALOMA (2)		
	LUGO SERRANO		
	LUGO MOHAVE		

Table 6 Probability of voltage collapse due to a fault on major 500kV transmission lines in the California subsystem (continued)

<i>No. Faulty line</i>	<i>Lines with exposed hidden relay failures</i>	<i>Probability of voltage collapse</i>	<i>Probability of VC for $p_f = 10^{-3}$, $p = 10^{-3}$</i>
12 DIABLO – MIDWAY (1)	DIABLO MIDWAY (2)	$p_f(p^3+p^4q+p^3q^2+p^3q^2) \approx p_f P^3$	$\approx 10^{-15}$
	DIABLO GATES		
	MIDWAY LOSBANOS		
	MIDWAY GATES		
	MIDWAY TEVATR		
	MIDWAY VINCENT (1)		
	MIDWAY VINCENT (2)		
	MIDWAY VINCENT (3)		
13 MIDWAY – VINCENT (1)	MIDWAY VINCENT (2)	$\approx p_f p^6$	$\approx 10^{-27}$
	MIDWAY VINCENT (3)		
	LOSBANOS MIDWAY		
	GATES MIDWAY		
	DIABLO MIDWAY (1)		
	DIABLO MIDWAY (2)		
	TEVATR MIDWAY		
	LUGO VINCENT (1)		
	LUGO VINCENT (2)		
	14 GATES – LOSBANOS		
GATES MIDWAY			
GATES DIABLO			
LOSBANOS MIDWAY			
LOSBANOS MOSSLAND			
15 GATES – DIABLO	TEVATR GATES	0	0
	LOSBANOS GATES		
	GATES MIDWAY		
	DIABLO MIDWAY (1)		
	DIABLO MIDWAY (2)		

8 Conclusions

Presently, there is a growing concern about the deterioration of the security of the US bulk power transmission system. The increasing number of brownouts and blackouts that have occurred recently in the USA clearly shows the need for new approaches in the security analysis of both planning and operation. It is perceived that N-1 contingency does not account for the detrimental role played by hidden relay failures in most blackouts.

This paper makes few additional steps towards the development of a practical methodology for a steady-state-risk assessment of multiple contingencies in large-scale power systems. In this regard, a statistical method for estimating the probabilities of hidden relay failures from historical data is presented and a collection of risk-assessment techniques and algorithms are described. In particular, they are able to pinpoint the weak links of a transmission network by identifying those lines whose tripping leads with the highest conditional probability of the loss of a large amount of load or of voltage collapse.

The weak links of a network need to be reinforced either by adding new transmission equipment or new intelligent adaptive control systems. The latter aims at mitigating the impact of a cascading failure via load and/or generator shedding and network splitting. They also aim at helping parts of the system to collapse in a graceful manner so that the duration of the interruption of service is reduced [36].

Acknowledgements

The authors acknowledge the support of the US Department of Defense and Electric Power Research Institute through the Complex Interactive Networks/Systems Initiative, WO 8333-01.

References

- 1 www.ari.vt.edu/workshop
- 2 Einhorn, M. and Siddiqi, R. (Eds.) (1996) *Electricity Transmission Pricing and Technology*, Kluwer Academic Publishers.
- 3 Tabors, R.T. (1996) 'Lessons from the UK and Norway', *IEEE Spectrum*, Aug., pp.45–49.
- 4 Rudnick, H. (1996) 'Pioneering electricity reform in South America', *IEEE Spectrum*, Aug., pp.38–44.
- 5 Ilic, M., Galiana, F. and Fink, L. (Eds.) (1998) *Power Systems Restructuring: Engineering and Economics*, Kluwer Academic Publishers.
- 6 Hunt, S. and Shuttleworth, S. (1996) 'Unlocking the grid', *IEEE Spectrum*, July, pp.20–25.
- 7 Amin, M. (2000) 'Toward self-healing infrastructure systems', *IEEE Computer Magazine*, August.
- 8 Hauer, J. and Dagle, J.E. (1999) *Consortium for Electric Reliability Technology Solutions Grid of the Future White Paper on Review of Recent Reliability Issues and system Events*, Office of Power Technologies, Assistant Secretary for Energy Efficiency and Renewable Energy, US Department of Energy, December.
- 9 Stoll, H.G. (Ed.) (1989) *Leat-Cost Electric Utility Planning*, John Wiley.

- 10 NERC Disturbance Reports – North American Electric Reliability Council, New Jersey, 1984-1988. Available at: <http://www.nerc.com/dawg/database.html>
- 11 Thorp, J.S., Phadke, A.G., Horowitz, S.H. and Tamronglak, S. (1998) ‘Anatomy of power system disturbances: importance sampling’, *Electrical Power & Energy Systems*, Vol. 20, No. 2, pp.147–152.
- 12 Thorp, J.S. and Phadke, A.G. (1999) ‘Protecting power systems in the post-restructuring era’, *IEEE Computer Applications in Power*, Jan., pp.33–37.
- 13 Baran, J. (1994) *Statistics for Long-Memory Processes*, Chapman & Hall.
- 14 Board of Review (1997) *First Phase Report: System Blackout and System Restoration*, Edison, 13-14 July.
- 15 Board of Review (1997) *Second Phase Report: System Blackout and System Restoration*, Con Edison, 24 August.
- 16 Wilson, G.L. and Zarakas, P. (1978) ‘Anatomy of a blackout’, *IEEE Spectrum*, Vol. 15, No. 2, Feb., pp.38–46.
- 17 IEEE/PSRC Working Group 13, ‘Transmission protective relay system performance measuring methodology’.
- 18 Efron, B. and Tibshirani, R.J. (1993) *An Introduction to the Bootstrap*. Chapman and Hall.
- 19 Mooney, C.Z. and Duval, R.D. (1993) *Bootstrapping: a Nonparametric Approach to Statistical Inference*. Sage Publications.
- 20 Kumamoto, H. and Henley, E.J. (1996) *Probabilistic Risk Assessment and Management for Engineers and Scientists*, 2nd ed., IEEE Press.
- 21 IEEE/PSRC Working Group 13, ‘Transmission protective relay system performance measuring methodology’, Submitted for publication.
- 22 Rubinstein, R.Y. (1981) *Simulation and the Monte Carlo Method*, John Wiley.
- 23 Cochran, W.G. (1977) *Sampling Techniques*, John Wiley.
- 24 Oliveira, G.C., Pereira, M.V.F. and Cunha, S.H.F. (1989) ‘A technique for reducing computational effort in Monte-Carlo based composite reliability evaluation’, *IEEE Transactions on Power Systems*, Vol. 4, No. 4, Oct., pp.1309–1315.
- 25 Savaderi, L. and Billinton, R. (1985) ‘A comparison between two fundamentally different approaches to composite system reliability evaluation’, *IEEE Transactions on PAS*, Vol. PAS-104, No. 12, Dec., pp.3486–3492.
- 26 Khan, M.E. and Billinton, R. (1992) ‘A hybrid model for quantifying different operating states of composite power systems’, *IEEE Transactions on Power Systems*, Vol. 7, No. 1, Feb., pp.187–193.
- 27 Sankarakrishnan, A. and Billinton, R. (1995) ‘Sequential Monte Carlo simulation for composite power system reliability analysis with time varying loads’, *IEEE Transactions on Power Systems*, Vol. 10, No. 3, Aug., pp.1540–1545.
- 28 Marnay, C. and Strauss, T. (1991) ‘Effectiveness of antithetic sampling and stratified sampling in Monte Carlo chronological production cost modeling’, *IEEE Transactions on Power Systems*, Vol. 6, No. 2, May, pp.669–675.
- 29 Nayheh, A.H. and Balachandran, B. (1995) *Applied Nonlinear Dynamics: Analytical, Computational, and Experimental Methods*, Wiley Interscience.
- 30 Canizares, C.A. and Alvarado, F.L. (1993) ‘Point of collapse and continuation methods for large scale AC/DC Systems’, *IEEE Trans. on Power Systems*, Vol. 8, No. 1, Feb., pp.1–8.
- 31 Irisarri, G.D., Wang, X., Tong, J. and Mokhtari, S. (1997) ‘Maximum loadability of power systems using interior point non-linear optimization method’, *IEEE Trans. on Power Systems*, Vol. 12, Feb., pp.162–172.
- 32 Chiang, H-D., Shah, K.S. and Balu, N. (1995) ‘CPFlow: a practical tool for tracing power system steady-state stationary behavior due to load and generation variations’, *IEEE Transactions on Power Systems*, Vol. 10, No. 2, May, pp.623–634.

- 33 Kubicek, M. and Marek, M. (1983) *Computational Methods in Bifurcation Theory and Dissipative Structure*. Springer-Verlag.
- 34 Ajjarapu, V. and Christy, C. (1992) 'the continuation power flow: a tool for steady state voltage stability analysis', *IEEE Transactions on Power Systems*, Vol. 7, No. 1, Feb., pp.416-423.
- 35 Tamronglak, S. (1994) 'Analysis of power system disturbances due to relay hidden failures', *PhD Thesis*, Virginia Polytechnic Institute and State University, March.
- 36 Adibi, M.M. (2000) *Power System Restoration: Methodology and Implementation Strategies*, IEEE Press.